IET Wireless Sensor Systems

Research Article

IET Journals
The Institution of Engineering and Technology

Impact of on-body IMU placement on inertial navigation

ISSN 2043-6386
Received on 15th July 2017
Revised 10th October 2017
Accepted on 1st November 2017
doi: 10.1049/iet-wss.2017.0087
www.ietdl.org

Nicolò Strozzi[1] ✉, *Federico Parisi*[1], *Gianluigi Ferrari*[1]

[1]*IoT Lab, Department of Engineering and Architecture, University of Parma, Via Parco Area delle Scienze 181/A, Parma, Italy*

✉ *E-mail: nicolo.strozzi@studenti.unipr.it*

Abstract: Even though technology-aided personal navigation is an extensively studied research topic, approaches based on inertial sensors remain challenging. In this study, the authors present a comparison between different inertial systems, investigating the impacts of on-body placement of Inertial Measurement Units (IMUs) and, consequently, of different algorithms for the estimation of the travelled path on the navigation accuracy. In particular, the system performance is investigated considering two IMU placements: (i) on the feet and (ii) on the lower back. Sensor fusion is then considered in order to take advantage of the strengths of each placement. The results are validated through an extensive data collection in indoor and outdoor environments.

1 Introduction

Personal navigation is a well-studied research field, in which different hardware and software solutions have been adopted. Many approaches based on Inertial Measurement Units (IMUs) have been proposed in recent years but the intrinsic limitations of inertial sensing technologies, such as the measurement drift, make their performance still non-comparable with navigation systems that rely on external infrastructures. The use of technologies based on radio signals, such as ultra-wide band (UWB), WiFi, or Bluetooth, has been widely investigated for both the design of stand-alone localisation systems [1, 2] and the reduction of errors in the inertial estimates [3, 4]. These kinds of solutions, usually achieve good performance but their infrastructure dependency, high maintenance costs, and low flexibility make them inadequate for many practical applications. On the other hand, approaches based on Global Navigation Satellite Systems (GNSSs), such as GPS or Galileo [5, 6], are very effective in outdoor scenarios but perform very poorly in indoor environments or in applications where high rate positioning estimation is needed. Finally, methods relying on cameras and computer vision enable highly accurate reconstruction of body movements in three-dimensional (3D) space [7], but they have many drawbacks, such as high costs, occlusion problems, and limited acquisition volume.

Solutions based on inertial sensing can provide several advantages because of their infrastructure independence, flexibility, cost effectiveness, portability, and the possibility to attach sensors directly to the subject's body. Unlike radio technologies, the inertial sensing technologies are subject to different errors (e.g. drift, incorrect sensors' positioning, per-subject calibration), which need to be reduced using specific correction techniques in order to make the measurements reliable. Most of these error reduction strategies depend on the sensors' positioning on the subject's body.

In our previous works [8, 9], we investigated the impact of two specific IMUs' placements (namely on the subject's feet and lower back) on the performance of purely inertial navigation systems. In this paper, we focus on the analysis of the strengths and weaknesses of the previously developed solutions and propose novel hybrid methods, which combine data from IMUs placed on different body segments to improve the accuracy and reliability of the overall pedestrian navigation system.

This paper is organised as follows. In Section 2, an overview of navigation systems proposed in the literature is given, highlighting the innovation introduced by our work. In Section 3, an overview of the two navigation systems, based on the use of a single sensor's is presented. In Section 4, the novel method based on sensor fusion is analysed, emphasising strengths and weakness. In Section 5, experimental results are presented, considering both indoor/outdoor scenarios and estimating the computational costs of the proposed solutions. Finally, in Section 6 conclusions are drawn.

2 Related works

The advances in Micro Electro-Mechanical System (MEMS)-based inertial sensors have enabled the development of new motion analysis methods to accurately reconstruct a subject's movement in 2D or 3D spaces, without the use of external infrastructures and with reasonable costs. The personal navigation research field has widely benefitted from this evolution.

The first attempts to develop navigation systems based on MEMS-based inertial systems exploited foot's movement characteristics during the gait in order to limit the drift. In recent years, several solutions based on foot-mounted sensors have been proposed [10–12]. By using this particular sensor placement, it is possible to achieve an accurate gait segmentation and to apply the Zero velocity UPdaTe technique (ZUPT), which consists in resetting the estimated velocity when the foot is still on the ground: this allows reducing the drift. By using this method, it is also possible to increase the step length estimation accuracy, since the travelled distance between a stance phase and the next one can be estimated through direct integration of the de-drifted foot velocity. The main drawbacks of this algorithm are the fast orientation changes involved in the foot movement, which may introduce errors in the IMU's measurements. Moreover, sudden fluctuations may degrade the performance of orientation filters, which usually fuse data from different sensors (namely, accelerometer, gyroscope, and magnetometer) in order to compute reliable 3D orientations: this leads to error accumulation in the estimation of a pedestrian's travelled path. In [13], Jimenez *et al.* analyse different pedestrian navigation systems, highlighting the advantages of sampling the heading angle, measured with a foot-mounted sensor during the stance phase of gait, with respect to double integrating the acceleration to derive both step length and walking direction. Nevertheless, we remark that foot orientation is not always aligned with the subject's movement direction.

The placement of a single IMU on the lower back, close to the centre of mass (CoM) of the body, is a widely adopted approach to the design of pedestrian navigation systems. In fact, in this position the sensor's movements are highly dependent on the trunk's biomechanical characteristics and, therefore, are limited with respect to those acquired by the foot-mounted sensor. During gait, the heading angle measured through trunk positioned sensors (i.e.

a

b

Fig. 1 *Sensor positions: (a) the IMUs are mounted under the shoe-laces, one per foot; (b) the IMU is attached to a velcro band in the middle of the back, over the spine*

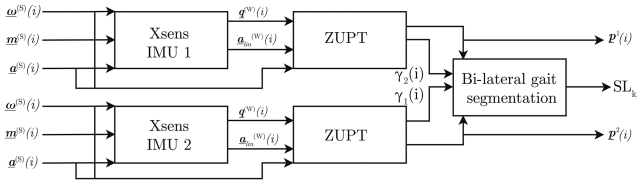

Fig. 2 *Block diagram of the EPDR algorithm for foot mounted IMU*

on the lower back, on the chest, on the pelvis etc.) is smoother and more representative of the actual movement direction [14]. The estimation of the travelled path in navigation systems based on trunk-mounted sensors is achieved by sampling the heading angle and updating the position propagating the steps' lengths along the estimated walking direction [14, 15]. The main limitation of this class of algorithms is the accuracy in the step length estimation. Several approaches have been investigated in order to correlate the signals measured from a trunk-mounted IMU with the frontal displacement [16–18]. The absence of a zero velocity phase and the poor results obtained by direct integration techniques have led to the development of empirical formulae, which usually correlate the vertical acceleration/displacement of the trunk with the frontal movement. Even though these methods have shown an adequate accuracy in many applications, they are not ideal for pedestrian navigation because of (i) the typically long duration of the task, which may lead to error accumulation, and (ii) the need of a per-subject calibration procedure.

The novelty of our work consists in combining the strengths of foot-mounted and trunk-mounted IMU-based navigation techniques in order to achieve a better estimate of the subject travelled path.

3 Inertial navigation algorithms

The placements of IMUs on the feet (as shown in Fig. 1*a*) or on the lower back, close to the CoM, (as shown in Fig. 1*b*) are commonly adopted strategies in order to exploit the biomechanical characteristics of the human body to facilitate purely inertial navigation for pedestrians.

In order to improve position estimations accuracy, to reduce drift, and to limit the number of used sensors, we adopt a Pedestrian Dead Reckoning (PDR) approach to the design of novel navigation algorithms. A PDR algorithm includes the following three main phases: (i) orientation estimation, (ii) step detection, and (iii) step length calculation. Our previous works focused on analysing separately pedestrian navigation systems relying on different sensor placements [8, 9]. In this section, we recall the last two phases of the PDR approach for the two navigation algorithms proposed in [8, 9], considering the placement of the sensors on the foot and on the lower back.

3.1 Experimental setup

In [8, 9], the proposed navigation algorithms rely on the use of Shimmer IMUs [Shimmer IMUs: https://www.shimmersensing.com.]. In this work, we utilise MTw Awinda IMUs by Xsens [Xsens IMUs: https://www.xsens.com/.]: in this case, the orientation estimation is directly computed on-board by the Xsens IMU. The high accuracy of the Xsens orientation estimation (with the proprietary algorithm) allows focusing on the (subsequent) design of inertial navigation algorithms.

The data stream generated by every IMU is transmitted to the Xsens Dongle, which is connected to a hand-held laptop. The online system performance is monitored through a Matlab® an application that collects and analyses the data in real time.

3.2 Foot-mounted sensor

By using the data collected by the sensor placed on the foot, as shown in Fig. 1*a*, it is possible to directly correlate the foot movement to the acceleration measured by the IMU. The standard approach to estimate the foot displacement consists in double integrating the linear acceleration – namely, the acceleration transformed from the body frame to the global frame by rotating the reference system and removing the gravity component. Mathematical details of this approach are presented in [8]. In particular, the first step of this procedure consists in segmenting the gait on the basis of the detection of the stationary phase of a stride using the following equations:

$$\begin{aligned} |\omega(i)| &= \sqrt{\omega_x(i)^2 + \omega_y(i)^2 + \omega_z(i)^2} \\ a_\Sigma(i) &\triangleq |a_{x,\mathrm{lin}}(i) + a_{y,\mathrm{lin}}(i) + a_{z,\mathrm{lin}}(i)| \end{aligned} \tag{1}$$

where $|\omega(i)|$ is the Euclidean module of the angular velocity and $a_\Sigma(i)$ is the absolute value of the sum of the tri-axial acceleration components.

The block diagram of the used Enhanced-PDR (EPDR) algorithm is shown in [8, Fig. 4] and includes all the three fundamental phases recalled at the beginning of this section. This algorithm refers to one sensor but can be applied separately to the case with sensors on both feet (with one IMU per foot), as shown in the block diagram in Fig. 2. While in [8] the orientation is estimated through the Madgwick algorithm [19], in the current system the Xsens IMU can directly and accurately estimate the linear acceleration. As shown in Fig. 2, this allows to directly use the ZUPT algorithm and segment the gait in its constituent phases – in fact, the signals computed through (1) are approximately equal to zero when the foot is stationary.

Define the following indicator sequence [8]:

$$\gamma(i) = \begin{cases} 1 & \text{if } \ a_\Sigma(i) < \mathrm{th}_a,\ |\omega(i)| < \mathrm{th}_\omega \\ 0 & \text{otherwise} \end{cases} \tag{2}$$

where $i = 1, 2, \ldots$ represents the sampling epoch. In other words, $\gamma(i) = 1$ when a_Σ and $|\omega|$ are below two heuristically chosen thresholds, denoted as th_a and th_ω, respectively. Additionally, we perform a check on the duration of each central stance phase, identifying the first and the last samples, in order to avoid the identification of false positive swing phases. According to this approach, for the jth central stance phase ($j = 1, 2, \ldots$), the starting and the ending samples are denoted, respectively, as $i_{\mathrm{start}}^{(j)}$ and $i_{\mathrm{end}}^{(j)}$: the corresponding central stance duration can be expressed as $T^{(j)} = t(i_{\mathrm{end}}^{(j)}) - t(i_{\mathrm{start}}^{(j)})$. In order to avoid considering spurious peaks, we discard the central stance phases with durations shorter than a

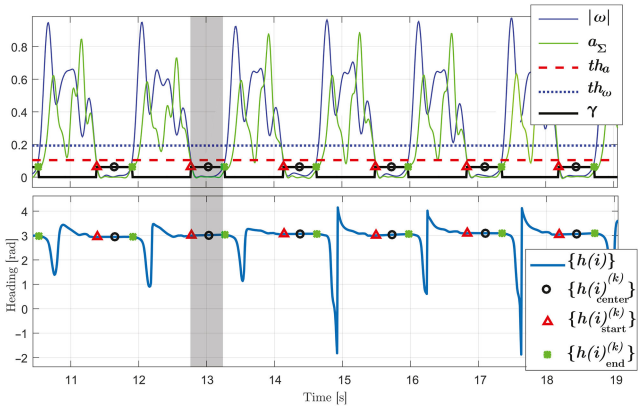

Fig. 3 *In the first plot, the signals a_Σ and |ω| and the corresponding thresholds th_a and th_ω are shown. Data are normalised for the sake of visualisation. Furthermore, the indicator signal γ, with values equal to 1 during central stance phases and to 0 during non-stationary phases, is visualised. In the second plot, the heading signal is shown, highlighting the steps detected through the stationary routine. In grey, a central stance phase is highlighted*

Fig. 4 *Walking human dynamic: heading angle*

proper threshold T_{min}. If $T^{(j)} < T_{\text{min}}$, than the indicator sequence $\{\gamma(i)\}$ is updated setting to zeros the corresponding samples (from $i = i^{(j)}_{\text{start}}$ to $i = i^{(j)}_{\text{end}}$ of the discarded jth central stance phase). On the basis of the experimental analysis carried out in [8], proper values of the considered thresholds are $\text{th}_\omega = 50$ rad/s; $\text{th}_a = 9$ m/s^2; and $T_{\text{min}} = 0.3$ s, respectively. The result of this stationary detection procedure is shown in the upper plot of Fig. 3. Considering only the swing phases, one can integrate the linear acceleration $\{\underline{\boldsymbol{a}}^{(\text{W})}_{\text{lin}}(i)\}$ and obtain the linear velocity $\{\underline{\boldsymbol{v}}^{(\text{W})}(i)\}$ by applying ZUPT.

At this point, the length of the kth stride is calculated by integrating the velocity $\{\underline{\boldsymbol{v}}^{(\text{W})}(i)\}$ between the end of a still phase (at epoch $i^{(j)}_{\text{end}}$) and the beginning of the following one (at epoch $i^{(j+1)}_{\text{start}}$). The linear acceleration double integration is performed by using the method presented in [9], namely by integrating the entire foot trajectory, in order to properly estimate the direction changes during the strides. The integration is performed only over the x and y coordinates, as our focus is on 2D navigation.

3.3 Lower back mounted sensor

When the sensor is placed in the trunk (lower back) of the test subject, it is very challenging to reconstruct the displacement in the frontal plane directly integrating the signal. For this reason, several approaches have been developed to correlate the dynamics of the CoM with the displacement of the entire body. We previously adopted the algorithm described by the block diagram in [8, Fig. 2]. This algorithm, denoted as De-Drifted Propagation (DDP), estimates the step length through the Weinberg model [16] and computes the travelled path by sampling the heading in the instant corresponding to the trunk vertical acceleration peaks. Other well-known algorithms for step length estimation, such as those developed by Zijlstra and Hof [17] and Gonzalez *et al.* [18], rely only on a single trunk-mounted sensor and usually achieve good accuracy. However, given the empirical nature of these models and the subject-dependent calibration required to tune the associated navigation algorithms, they often introduce errors in the final estimated path. To avoid these problems and obtain a more accurate step length estimation, in Section 4, we propose a hybrid approach which combines the accurate step length computed from the foot-mounted sensors with the robust heading angle measured through the trunk-mounted sensor.

4 Sensor fusion

In the previous section, it has been shown that the two chosen sensors' positionings (namely, foot and CoM) allow us to design different algorithms which exploit the peculiar motion dynamics of foot and trunk, respectively. In this section, the details of a novel hybrid method, which exploits the advantages of both sensors' positions, are presented. In particular, we focus on the analysis of different approaches to sample the heading angle and on the reconstruction of the travelled path using the step lengths computed with the algorithms described in Section 3. Moreover, the body displacement computed by the sensor on the back, due to the used empirical formulae, is not so accurate because of the dependency on the test subject characteristics, as shown in [8].

4.1 Heading sampling

The first phase of sensor fusion involves the synchronisation of data streams and the selection of sampling instants. In particular, the latter operation is necessary because of the body, during a normal walk, moves by following the patterns illustrated in Fig. 4. This typical oscillatory behaviour is captured by the heading angle measured by the sensor on the lower back, as shown in Fig. 5, which is directly compared to the one computed from the foot mounted sensor. It is possible to notice that the foot orientation varies consistently (with fluctuations approximately four times wider) with respect to the 'specular estimate' computed from the sensor on the lower back. By using, as a reference, the gait segmentation provided by the algorithm relying on the foot mounted sensors, the instants at which the body is aligned with the walking direction can be identified by analysing the heading angle of the trunk mounted sensor, as shown in Fig. 6. In particular, we choose to select the middle swing instant (namely, the instant between a stance phase and the corresponding contra-lateral one) to sample the heading angle because, as evidenced by Figs. 4 and 6, it corresponds to the instant at which the body very likely heads towards the walking direction. Using the gait segmentation information obtained through the EPDR algorithm, the middle swing instant and the corresponding heading sample (in quaternions notation) are computed as follows:

$$\begin{aligned} t(i^{(k)}_{\text{mid}}) &= \frac{t(i^{(k)}_{\text{end}}) + t(i^{(z)}_{\text{start}})}{2} + t(i^{(k)}_{\text{end}}) \\ \hat{q}(k) &= \text{median}\left(q\left[t(i^{(k)}_{\text{mid}}) - \frac{Win}{2F_s}, t(i^{(k)}_{\text{mid}}) + \frac{Win}{2F_s}\right]\right) \end{aligned} \tag{3}$$

where $t(i^{(k)}_{\text{mid}})$ is the middle swing instant; $t(i^{(k)}_{\text{end}})$ is the end stance time of the kth right step; $t(i^{(z)}_{\text{start}})$ is the start stance time of the zth left step; median is the median function, defined as the middle value in a sorted dataset (if the samples' number is even, the mean of the two central values in the dataset is used); q are the quaternions collected by the back sensor; $\hat{q}(k)$ are the quaternions sampled with the proposed method for the kth step; *Win* is the number of samples over which the median heading is calculated, and F_s is the sampling frequency (dimension: Hz). In our experiment setup, we set *Win* to ten samples.

However, if the gait segmentation provided by the foot sensor is not available, an alternative method for sampling the heading angle is proposed. It consists of intersecting the heavily low-pass filtered version of the heading signal with its original (unfiltered) version. By using this technique, one can find the same middle swing point as the central instant of the heading excursion, as shown in Fig. 7. The filter used to obtain the heavily filtered heading has to be a finite impulse response (FIR) filter, in order to perform a near real-time analysis. This type of filtering introduces a fixed delay equal to $M/2$ samples, where M is the number of taps used by the filter. In our case, we use an FIR filter designed by using the least squares approach, namely by minimising the discrepancy between a specified arbitrary piecewise-linear function and the filter's

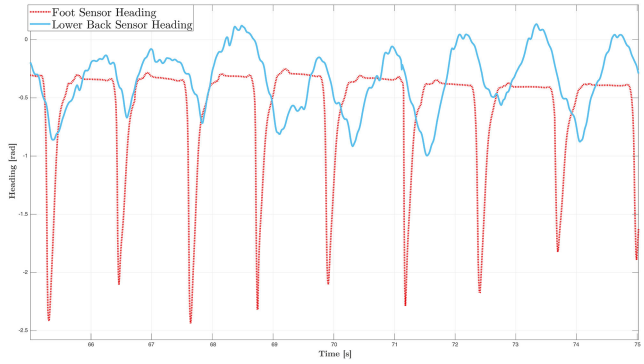

Fig. 5 *Comparison between the heading angles measured through the foot sensor (red line) and the lower back sensor (blue line)*

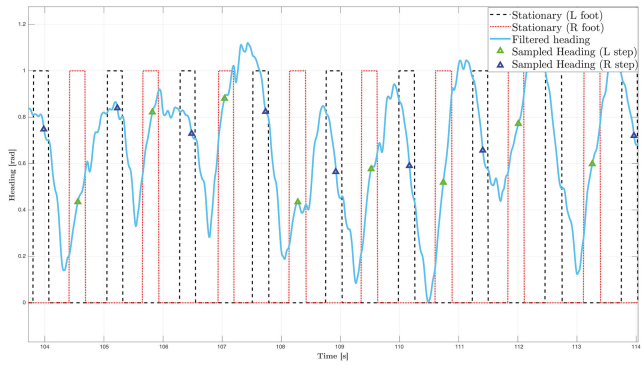

Fig. 6 *Heading estimated from the trunk-mounted (lower back) sensor compared with the stance phases identified through the feet mounted sensors*

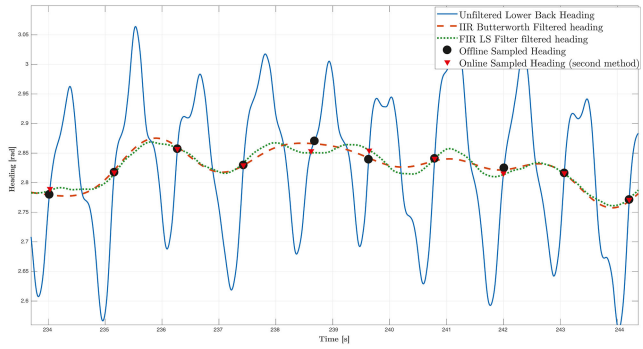

Fig. 7 *Heading provided by the lower back sensor is sampled according to the second method. The intersections between the heading signal filtered through the FIR filter and the original signal are shown as red triangles. For comparison, the same procedure is carried out with an offline IIR filter and the intersections are shown as black dots*

magnitude response. The other parameters of the filter are (i) the passband frequency, set to 0.5 Hz, and (ii) the stopband frequency, set to 0.6 Hz.

The two proposed segmentation methods are developed in order to identify very precisely the middle swing instant and, consequently, their accuracy has to be comparable. In spite of that, these methods are not completely equivalent. In particular, there are the following two main weaknesses that affect the second method (i.e. the method which exploits the filtered heading to identify the correct sampling instants) with respect to the gait segmentation based on the data collected from the feet mounted sensors.

- Changes in the walking pattern (i.e. turnings, velocity changes, obstacle avoidance etc.) cause irregular heading variations: this leads to a misalignment between the intersection of the two signals (filtered and unfiltered heading) and the middle swing instant.
- The filter introduces a delay with respect to the sampling instant detection. In fact, in order to obtain the signal shown in Fig. 7, we set $M = 150$ samples which, for a sampling rate $F_s = 100$ Hz, corresponds to a delay equal to $M/2 \cdot 1/F_s = 750$ ms. In order to perform a near real-time orientation sampling, the system needs to initially store 750 ms of data and, then, by taking into account the delay, to use the filter to obtain the correct sampling instant.

For comparison purposes, this technique has been tested with an infinite impulse response (IIR) filter, namely, a sixth-order low-pass Butterworth filter with a cut-off frequency equal to 0.5 Hz, applied offline to the entire unfiltered heading signal. The resulting signal (red dashed line in Fig. 7) is then compared with the one obtained by the FIR filter, shifted backwards by $M/2$ samples (corresponding to the filter delay). As can be seen in Fig. 7, the IIR filter and the FIR filter lead to a comparable performance with respect to the middle swing instant identification: the average error, between the two heading angles estimated by using the two filters, is equal to only 0.03 rad.

In conclusion, when the gait segmentation provided by the feet mounted sensors is available, its adoption has to be preferred. If the feet sensors' segmentation information is not available but the step length estimation is provided (e.g. an external step length estimation system with no gait segmentation information is available), the second method represents a good option. In general, the two methods show a substantial correspondence between the two sampling instant estimates.

4.2 Step propagation

Once the orientation has been sampled, it is possible to reconstruct the travelled path by propagating the measured frontal displacement (corresponding, in this case, to the step length estimates provided by the foot mounted sensors) in the direction indicated by the sampled heading angle. In particular, the estimated path can be computed using the following equations:

$$\begin{aligned} h(k) &= \arctan 2(2(\hat{q}_0(k)\hat{q}_3(k) + \hat{q}_1(k)\hat{q}_2(k)) \\ &\quad , \ldots, 1 - 2(\hat{q}_2^2(k) + \hat{q}_3^2(k))) \\ p^{(x)}(k) &= \cos(h(k)) \times SL_k + p^{(x)}(k-1) \\ p^{(y)}(k) &= \sin(h(k)) \times SL_k + p^{(y)}(k-1) \end{aligned} \tag{4}$$

where $\hat{q}(k)$ is the lower back orientation sampled by applying one of the methods described in Section 4.1; $h(k)$ is the corresponding heading angle in Euler notation; $(p^{(x)}(k), p^{(y)}(k))$ is the estimated position at the kth step; and SL_k is the length of the kth step estimated through the feet sensors. The $\arctan 2(x, y)$ function allows converting the orientation from quaternion notation to Euler notation, in order to obtain the heading in the $[-\pi, \pi]$ range. Once the heading angle is computed, though the trigonometric formula in (4), is it possible to estimate the displacement along the x and the y axes.

5 Results

In order to estimate the system performance, outdoor and indoor scenarios are considered. In each case, a reference path is selected. By introducing checkpoints along the chosen paths, one can evaluate the position estimation error of the proposed navigation algorithm as a function of the travelled distance. More precisely, we evaluate the position error, in terms of both absolute error ϵ^a (dimension: m) and relative error ϵ^r (dimension: %) with respect to the actual travelled path. In the following, the mean (absolute and relative) errors between the estimates obtained by applying the EPDR algorithm to the right and the left foot are shown. The obtained results are presented by distinguishing between outdoor and indoor scenarios.

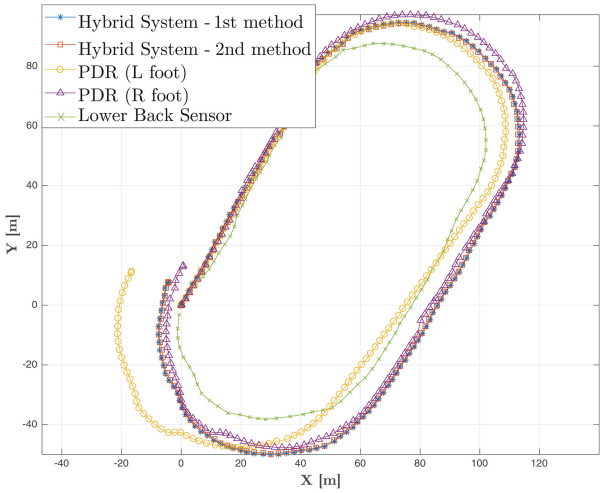

Fig. 8 *Comparison between the paths estimated by: (i) the EPDR algorithm applied on the right (yellow line with circles) and the left (purple line with triangles) feet; (ii) the DDP method based on a single lower back sensor (green line with crosses); (iii) the first hybrid algorithm, which samples the lower back heading through the mid swing method (blue line with stars) and the second hybrid algorithm, which samples the lower back heading by using the intersection between filtered and unfiltered heading signal (red line with squares)*

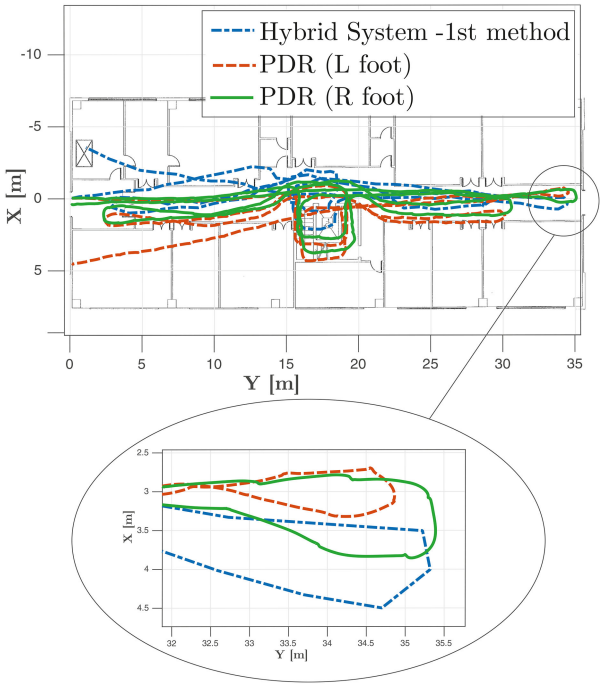

Fig. 9 *Comparison, in the indoor environment, between the path estimated by the EPDR (red dashed line for the left foot and green solid line for the right foot) and the hybrid (blue dashed-dotted line) systems. In the bottom of the figure, we zoom a detail of the reconstructed path, which shows the impact of the step propagation on the measured error*

5.1 Outdoor scenario

The outdoor experimental evaluation has been carried out on the athletic track of the campus of the University of Parma, Italy. As shown in Fig. 8, the path is composed of two large and smooth curves and two straight lines. The reconstructed paths obtained by applying the EPDR algorithm on feet, the DDP method, and the hybrid approach (using the two proposed methods for sampling the heading angle) are shown. The absolute and relative estimation errors for each method are presented in Table 1.

The orientation computed from the lower back sensor is more stable and allows to obtain a better performance than that obtained with the feet mounted sensors. This is due to the fact that feet are subject to rapid orientation changes, even in a smooth track, and this leads to errors in the heading estimation. This performance is intuitively expected from the heading behaviour as shown in Fig. 5. The following results can be carried out:

- By looking at the performance in Table 1, it is possible to notice that the results obtained with the EPDR are less accurate (i.e. with higher error) than those estimated by the hybrid system (both methods, 1 and 2 have the same performance), although the same step length is used. As a consequence, during the first part of the track, the two systems present comparable values of the error ϵ. However, over a longer path, the estimate obtained using the lower back sensor orientation outperforms the one based on the EPDR system.
- The DDP system achieves very good performance in terms of orientation estimation (the final point is very close to the actual one and the general 'estimated shape' is correct) but, due to the empirical formulae used for the step length calculation, it underestimates the actually travelled path and is outperformed by the hybrid system, which relies on the more accurate step length estimates given by the EPDR algorithm.
- Finally, from Fig. 8 one can observe the correspondence between the two proposed heading sampling methods for the hybrid algorithm. Without loss of generality, in the following, we will present only performance results obtained through the EPDR method and the hybrid algorithm with the first heading sample technique.

5.2 Indoor scenario

In indoor environments, the step propagation technique generally used for path estimation with trunk mounted IMUs is less accurate than for outdoor path estimation, as we have already shown in [9]. In particular, as can be seen from Fig. 9, the sharp curves typical of indoor paths lead to the introduction of trajectory errors. These problems are caused by straight line propagation (i.e. step propagation) over multiple curves (long paths), and can lead to a relevant error accumulation. These problems also emerge from Table 2, in which the performance of the EPDR systems is slightly better than the one achieved by the hybrid system first method. This error affects not only our hybrid approach but, more generally, all the techniques in which, first, the orientation is computed and, then, the step displacement is propagated.

5.3 Relative error comparison

In Fig. 10, the relative error ϵ^r between the estimated path length and the true path length is shown as a function of the distance, considering the EPDR and the hybrid systems in both indoor and outdoor scenarios. From the results in this figure, it appears clear

Table 1 Performance, in terms of absolute and relative errors, of the considered algorithms in the outdoor scenarios

Distance, m	Foot IMU PDR (EPDR)		Hybrid system (first and second methods)		Lower back sensor (DDP)	
	ϵ^a, m	ϵ^r, %	ϵ^a, m	ϵ^r, %	ϵ^a, m	ϵ^r, %
84.4	1.5	1.8	0.4	0.47	1.2	1.42
200	5.2	2.6	3.3	1.65	6.9	3.45
284.4	7.3	2.6	4.7	1.65	8.4	2.95
400	12.9	3.23	7.6	1.9	2.7	0.67

Table 2 Performance, in terms of absolute and relative errors, of the considered algorithms in the indoor scenarios

Distance, m	Foot IMU PDR (EPDR)		Hybrid system (first and second methods)	
	ϵ^a, m	ϵ^r, %	ϵ^a, m	ϵ^r, %
36	0.6	1.7	1.1	3.1
54	1.2	2.2	1.7	3.1
81	1.7	2.1	2.5	3.2
93	1.9	2.0	3.3	3.5
105	2.7	2.5	3.9	3.7

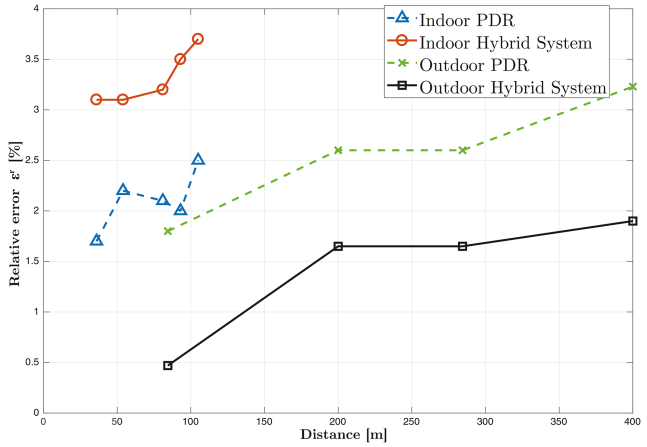

Fig. 10 *Relative error ϵ^r, as a function of the travelled distance, for the considered algorithms in both indoor and outdoor scenarios*

that in the indoor scenario the relative error increases more rapidly for both navigation systems, due to the error introduced by the sharp curves. Moreover, it is possible to notice that the EPDR system's estimated trajectory is more accurate than that of the hybrid system, in which the step propagation introduces smaller errors at every orientation change. The relative error in the outdoor scenario, instead, increases less rapidly and, due to the smooth changes in the heading angle, the hybrid system is more effective. In particular, the hybrid system reaches a very accurate estimation with a final error ϵ^r equal to 1.9% of the length of the total travelled path.

5.4 Computational costs

The proposed algorithms have been tested with a laptop equipped with an Intel i7-6700HQ processor working at 2.6 GHz, 8 GB RAM (DDR3, 1600 MHz) running Matlab® 2017a. In order to clarify the algorithm steps, a block diagram of the Matlab code is shown in Fig. 11. In particular, the algorithm is composed of the following main steps:

- *Controlled delay:* This block calculates the time spent in the previous cycle, in order to keep the delay between a data acquisition and the next one almost constant and equal to ~300 ms. By default, the time delay introduced by this block is equal to 270 ms (as, on average, the previous cycle lasts around 30 ms). If the previous cycle has lasted more time than usual (i.e. a step is detected), the time delay is consequently reduced.
- *Data acquisition (A):* Given that the Xsens system adopts an event-based approach to transmit every single data and taking into account that the navigation algorithm cannot perform a cycle every data packet, a custom library able to collect the data in a buffer has been implemented. Every sensor transmits the inertial data to a specified buffer. This part of the algorithm reads the data from these buffers and resets them.
- *Single sensor gait segmentation (B):* In this step, the foot phase (i.e. swing or stride) is analysed. If a stance phase is detected, the ZUPT algorithm is performed; otherwise, the foot is still in a swing phase and the algorithm returns at the acquisition step.
- *ZUPT (C):* In this block, the ZUPT algorithm is applied. The drift is removed from the measurements and the stride length is estimated. At this level, the data from every sensor are processed separately.
- *Bi-lateral gait segmentation (D):* In this block, the complete (bi-lateral) gait is analysed and segmented. The step length is computed by exploiting the two gait segmentation (i.e. the gait segmentations performed separately from the two feet sensors) and stride length estimations.
- *Sampling instant detection (E):* In this phase, one of the two methods presented in Section 4.1 is implemented. We refer as E1 to the sampling method based on the information provided by the foot sensors (method 1) and we use the notation E2 for the method based on the intersection between the filtered and unfiltered versions of the heading angle (method 2).
- *Step propagation (F):* In this final phase, the step lengths estimated through the feet mounted sensors and the heading signal from the lower back sensor sampled in the previous phase are fused in order to perform the navigation.

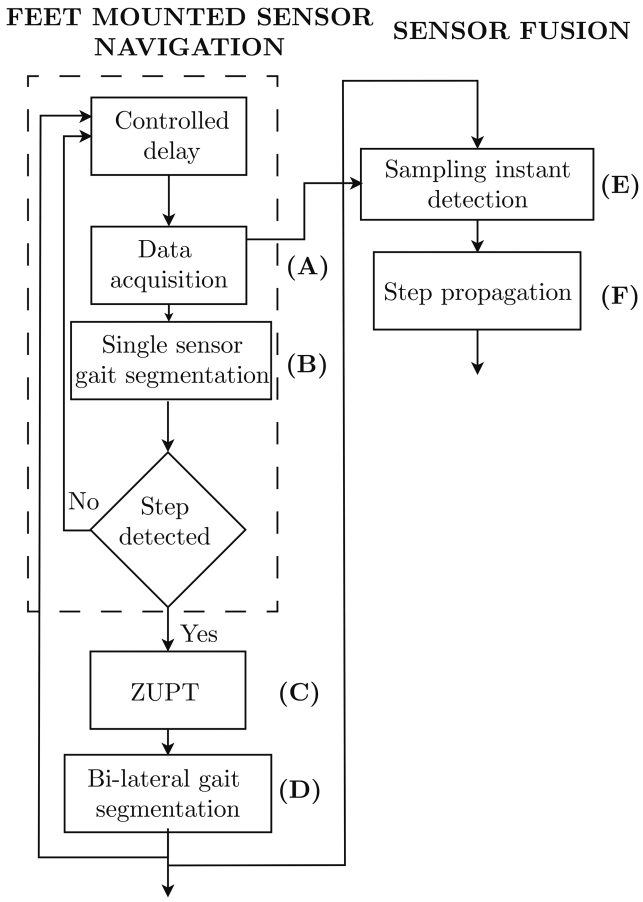

Fig. 11 *Flow diagram of the hybrid system operational steps*

The time necessary to perform every phase of the algorithm on the used laptop is presented in Table 3. It is important to highlight that because of the *Controlled delay* function, the number of acquired samples per sub-cycle is about 30: therefore, the procedures (A) and (B) are computed with this number of samples per sub-cycle. The subsequent tasks, instead, are computed every time a stride is detected. By using several acquisitions with a

Table 3 Computational cost organised per task (dimension: ms). These times refer to the processing load associated with a new step, which, on average, is detected every 600 ms

(A) three IMUs four sub-cycles	(B) two IMUs four sub-cycles	(C)	(D)	(E1)	(E2)	(F)
4.4	7.4	16.2	0.4	0.46	1.3	0.05

normal walking pace, we have measured a stride event, on average, every 1.2 s: this corresponds, for a sampling rate equal to 100 Hz, to a number of samples per stride equal to 121 ± 13 (i.e. the average value $\pm$ standard deviation). In Table 3, we show the computational time necessary to update the position, namely the time needed to process a double stride (i.e. a stride per foot), in order to perform the bi-lateral gait segmentation. More precisely: task (A) is executed four times per sensor every position update; task (B) is executed four times only for the feet mounted sensors; whereas tasks (C)–(F) are performed once per position update. Given that the average stride duration is 1.2 s, a position update is performed every step, i.e. on average, every 600 ms.

In conclusion, the total time necessary to perform a position update every 600 ms by the hybrid system (with the first heading segmentation method) is 28.91 ms: this definitely allows a real-time implementation of our approach.

6 Conclusions

In this paper, we have compared two different inertial navigation systems with the aim of investigating the strengths and weaknesses of various IMU placements in terms of 'quality' of inertial navigation. The obtained results show that the orientation collected from a sensor placed near the CoM, on the lower back, guarantees a more stable behaviour with respect to the orientation obtained from a sensor placed on the foot. On the other hand, step length estimation is more effective when the sensor is placed on the foot, due to direct double integration and ZUPT: at the opposite, navigation systems relying exclusively on a single sensor mounted on the trunk use empirical formulae to estimate the frontal body displacement. We have also developed a novel hybrid method, which exploits the advantages of the two sensor placements and achieves better or comparable performance in both outdoor and indoor environments. The main limitation of the latter method consists of the error introduced by the step propagation technique in the presence of sharp curves. The obtained results should be taken into account during the development of inertial navigation algorithms, in particular in the development of navigation algorithms with trunk-mounted and/or hand-held sensors.

In our future work, we aim at reducing the number of sensors necessary to perform sensor fusion, step length estimation, and gait segmentation. This will be achieved by removing a foot mounted sensor, thus trying to apply gait segmentation by assuming a gait symmetric model.

7 References

[1] Segura, M., Mut, V., Sisterna, C.: 'Ultra wideband indoor navigation system', *IET Radar Sonar Navig.*, 2012, **6**, (5), pp. 402–411

[2] Pagano, S., Peirani, S., Valle, M.: 'Indoor ranging and localisation algorithm based on received signal strength indicator using statistic parameters for wireless sensor networks', *IET Wirel. Sens. Syst.*, 2015, **5**, (5), pp. 243–249

[3] Fan, Q., Sun, B., Sun, Y.*, et al.*: 'Performance enhancement of MEMS-based INS/UWB integration for indoor navigation applications', *IEEE Sens. J.*, 2017, **17**, (10), pp. 3116–3130

[4] Hu, W.Y., Lu, J.L., Jiang, S.*, et al.*: 'WiBEST: a hybrid personal indoor positioning system'. Wireless Communications and Networking Conf. (WCNC 2013), Shanghai, China, 2013, pp. 2149–2154

[5] Misra, P., Enge, P.: '*Global positioning system: signals, measurements and performance*' (Ganga-Jamuna Press, Lincoln, 2010, 2nd edn.)

[6] Benedicto, J., Dinwiddy, S.E., Gatti, G.*, et al.*: '*Galileo: satellite system design and technology developments*' (European Space Agency (ESA), Noordwijk, NL, 2000)

[7] Camplani, M., Paiement, A., Mirmehdi, M.*, et al.*: 'Multiple human tracking in RGB-depth data: a survey', *IET Comput. Vis.*, 2017, **11**, (4), pp. 265–285

[8] Strozzi, N., Parisi, F., Ferrari, G.: 'On single sensor-based inertial navigation'. IEEE EMBS 13th Annual Int. Body Sensor Networks Conf. (BSN 2016), San Francisco, CA, 2016

[9] Strozzi, N., Parisi, F., Ferrari, G.: 'A multifloor hybrid inertial/barometric navigation system'. IEEE Int. Conf. Indoor Positioning and Indoor Navigation (IPIN 2016), Alcala de Henares, ES, 2016

[10] Beauregard, S., Haas, H.: 'Pedestrian dead reckoning:a basis for personal positioning'. Workshop on Positioning, Navigation and Communication (WPNC 2006), Hannover, Germany, 2006

[11] Fourati, H.: 'Heterogeneous data fusion algorithm for pedestrian navigation via foot-mounted inertial measurement unit and complementary filter', *IEEE Trans. Instrum. Meas.*, 2015, **64**, (1), pp. 221–229

[12] Hsu, Y.L., Wang, J.S., Chang, C.W.: 'A wearable inertial pedestrian navigation system with quaternion-based extended Kalman filter for pedestrian localization', *IEEE Sens. J.*, 2017, **17**, (10), pp. 3193–3206

[13] Jimenez, A.R., Seco, F., Prieto, C.*, et al.*: 'A comparison of pedestrian dead-reckoning algorithms using a low-cost MEMS IMU'. Intelligent Signal Processing (WISP 2009), Budapest, Hungary, 2009, pp. 37–42

[14] Alvarez, J.C., Alvarez, D., Lopez, A.M.*, et al.*: 'Pedestrian navigation based on a waist-worn inertial sensor', *Sensors*, December 2012, **12**, pp. 10536–10549

[15] Basso, M., Galanti, M., Innocenti, G.*, et al.*: 'Pedestrian dead reckoning based on frequency self-synchronization and body kinematics', *IEEE Sens. J.*, 2017, **17**, (2), pp. 534–545

[16] Weinberg, H.: 'Using the adxl202 in pedometer and personal navigation applications'. Analog Devices, 2002, Application Note AN-602

[17] Zijlstra, W., Hof, A.L.: 'Assessment of spatio-temporal gait parameters from trunk accelerations during human walking', *Gait Posture*, 2003, **18**, pp. 1–10

[18] Gonzalez, R.C., Alvarez, D., Lopez, A.M.*, et al.*: 'Modified pendulum model for mean step length estimation'. 2007 29th Annual Int. Conf. IEEE Engineering in Medicine and Biology Society, 2007, pp. 1371–1374

[19] Madgwick, S.O.H., Harrison, A.J.L., Vaidyanathan, R.: 'Estimation of IMU and MARG orientation using a gradient descent algorithm'. IEEE Int. Conf. Rehabilitation Robotics Rehab Week (ICORR 2011), ETH Zurich Science City, Switzerland, 2011, pp. 1–7